Japanese Journal of Applied Physics
Vol. 43, No. 2A, 2004, pp. L176–L179

Far-Infrared Resonance in Split Ring Resonators

A-Chuan HSU[1,2,*], Yi-Kai CHENG[1,2], Kuan-Hung CHEN[1,2], Jyh-Long CHERN[1,2], Shich-Chuan WU[3], Ching-Fu CHEN[3], Hao CHANG[4], Yu-Hung LIEN[4] and Jow-Tsong SHY[4]

[1]*Institute of Electro-Optical Engineering, National Chiao Tung University, Hsinchu 300, Taiwan, R.O.C.*
[2]*Microelectronics and Information System Research Center, National Chiao Tung University, Hsinchu 300, Taiwan, R.O.C.*
[3]*National Nano Device Laboratories, Hsinchu 300, Taiwan, R.O.C.*
[4]*Department of Physics, National Tsing Hua University, Hsinchu 300, Taiwan, R.O.C.*

(Received November 13, 2003; accepted November 17, 2003; published January 9, 2004)

We experimentally investigated the resonance effect of planar metallic split ring resonators (SRRs) in the far-infrared region (FIR) (~10.6 μm). Experimental results indicated that they exhibit resonance around 10.6 μm, implying negative permeability in the FIR region. Furthermore, the ratio of effective dimensions of the SRR cell and the wavelength of the incident beam was around 1 which suggested a wide scale independence. This size tolerance is useful in realizing the meta-materials with negative indices of refraction in the optical wavelength domain. [DOI: 10.1143/JJAP.43.L176]

KEYWORDS: split ring resonator patterns, meta-materials, resonance, negative permeability, far-infrared region, negative index

Meta-materials or composite meta-materials have attracted much interest in recent years because of their unique physical properties and novel applications to various fields in science and technology.[1–4] Two parameters, electric permittivity (ε) and magnetic permeability (μ), are deterministic for the materials in terms of their response to the electromagnetic radiation. In ordinary materials, both ε and μ are positive. However, very thin wires[5] may exhibit negative permittivity ($\varepsilon<0$), while a periodic array of split ring resonators (SRRs)[6] may have negative permeability ($\mu<0$) in the microwave region, in which both of the negative parameters are revealed by resonance (absorption of incident energy) at corresponding frequencies. The SRR pattern is key to realizing negative permeability and meta-materials with negative index of refraction (NIR) or left-handed meta-materials.[3,7] NIR meta-materials have potential applications in super-resolution optics where they may contribute to the breaking of the diffraction limit,[1,8] yielding important results in science and technology. However the SRR structures are realized in the microwave region from one to around 20 GHz. The optical wavelength region is of interest in exploring the fundamental and practical limitations of NIR meta-materials. In the microwave region, the mm-scaled SRR cell is easily fabricated, but fabrication in the optical wavelength region is difficult, since the SRR pattern must be scaled down to the nanometer scale in the optical wavelength region. Mean-field theoretical consideration indicates that the characteristic scale of SRR should be at least tens or few hundred times smaller than the incident wavelength. This requirement implies that the SRR cells should be treated as small-scale artificial molecules or atoms.[9] In this paper, we report the resonance of SRR in the wavelength of the far-infrared region (FIR) at ~10.6 μm and the scale of SRR can be as large as the wavelength. This scale tolerance could be important in realizing NIR meta-materials in the optical wavelength region.

The SRR pattern sample was fabricated by means of a standard IC process. Aluminum (Al) with ~0.5 μm thickness was deposited on the silicon (Si) substrate with ~0.7 mm thickness to construct the SRR pattern. Only the square SRR pattern is considered here and the geometry is shown in Fig. 1(a). The average size of each cell was 10.48 μm and the width of each metallic line was 1 μm. The horizontal separation between the two SRR cells was 3.2 μm and the vertical separation was 6.8 μm. On average, the area covered with SRR had a size of ~ 3.5 mm × 3.5 mm and the area covered by the laser beam included approximately 255 × 200=51,000 SRR cells that acted simultaneously because of the coherence of laser light. The structure of the SRR cell was determined by optical microscopy and is presented in Fig. 1(a).

Figure 1(b) presents the experimental setup. A linear polarized light source from a laboratory-built CO_2 laser was separated into two beams: one was guided to the sample and the other was used for reference, and their energy separation ratio was approximately 9:1. A polarizer (GTE Sylvania, model 485) was inserted in the front of the sample. The polarization ratio of the s-polarization to the p-polarization was measured as 1000:3, such that the stronger $\boldsymbol{E}$ field orthogonal to the optical axis was on the y-axis, as depicted in Fig. 1(c). The output beam profile was transverse electromagnetic mode, TEM_{00}, determined by using a thermal image plate for CO_2 lasers (Macken Instruments, 22-A/22-B). The propagation of energy given by the Poynting vector $\boldsymbol{S}$, which is effectively the same as the wave vector $\boldsymbol{k}$ here, is parallel to the optical axis. In the experiment, the output power of the CO_2 laser was normally over 4 W. The diameter of the optical beam on the sample was 4 mm, and was controlled using a diaphragm. The loss of energy due to the blocking by the diaphragm was fixed in the experiment and the intensity on the sample was typically around 100 mW. The sample was air-cooled to prevent thermal damage to the metal Al. The transmitted power was measured using an IR detector (Scientech, 36–001; spectral range 0.25–35 μm). In the experiment, the transmitted power of the transmitted beam (P2) was normalized with the power of the monitored beam (P1) to prevent any influence of the fluctuation in power from the CO_2 laser, such that all data were comparable.

A local coordinate system (x, y, z) is used herein, where the z-axis corresponds to the normal axis of the SRR sample, i.e., the normal direction of the sample penetrated through the ring. When the sample was orientated for normal incidence, the optical axis is parallel to the z-axis; rotating the sample through 90 degrees oriented the optical axis perpendicular to the z-axes, as indicated in Fig. 1(c). The

*E-mail address: achsu@faculty.nctu.edu.tw

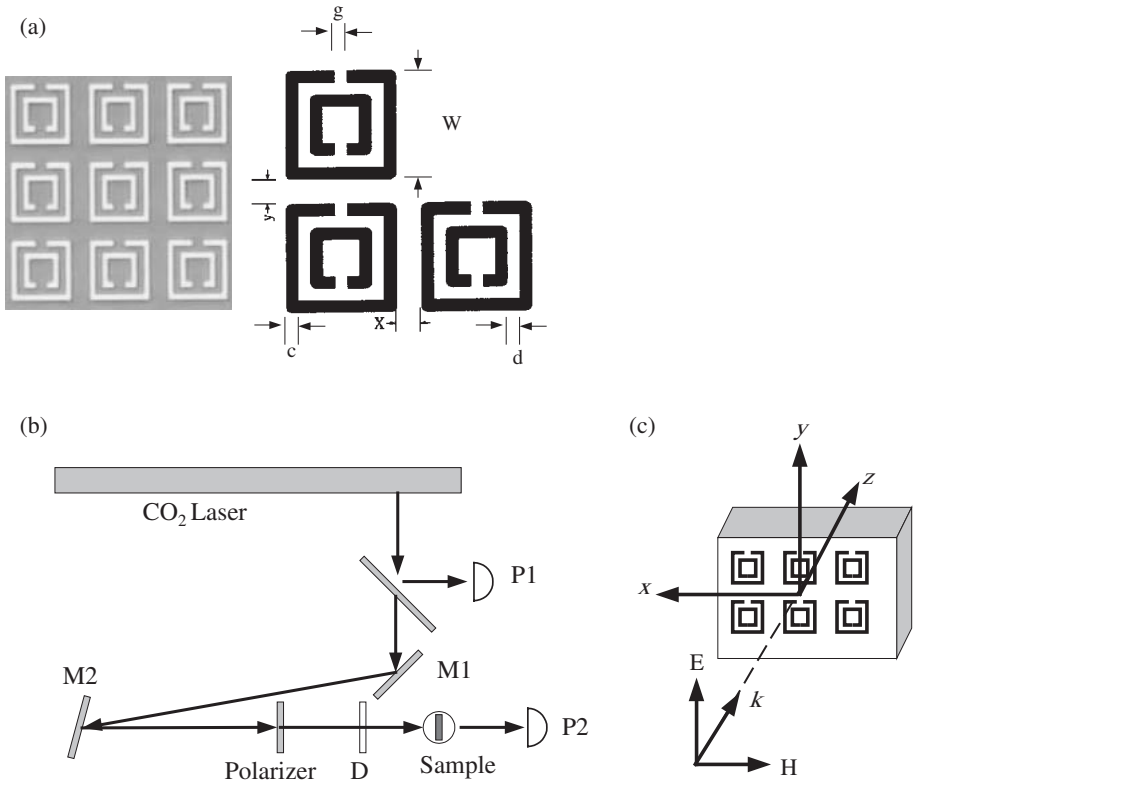

Fig. 1. (a) SRR pattern observed by optical microscopy. The scale was c=1.0 μm, d=1.2 μm, g=1.84 μm, w=10.48 μm, X=3.2 μm, and Y=6.8 μm; (b) experimental setup and (c) relationship of orientation between the propagation direction $\boldsymbol{k}$, the electric field $\boldsymbol{E}$ and the magnetic field $\boldsymbol{H}$ of the incident beam and the sample.

sample was symmetrically rotated about the y- and x-axis. For comparison, the transmission curves at two wavelengths, 10.86 μm and 9.43 μm, were measured. These two laser wavelengths were considered because the characteristic dimensions of the SRR cells were in between these two wavelengths. The Si substrate was grown by Czochralski pulling techniques and exhibits a strong absorption at 9 μm. At 10.86 μm, the transmission of a *pure* Si sample is ∼38%, while at 9.43 μm, it is ∼40%.

The angular distribution of transmission caused by the SRR cells was measured. The vertical axis, "normalized transmission", represents the ratio of the power detected after the light beam propagates through the (tilted) sample to that before it. The incident power from the detected P1 was calculated as shown in Fig. 1(b), and the power passing through the polarizer and the diaphragm was included. Notably, this configuration is preferred because it ensures that the polarization of the incident beam on the sample can be well controlled without affecting the beam splitter and mirror. The tilt angle of the sample with respect to the y-axis is denoted by θ. At normal incidence, θ=0, the incident beam is normal to the sample, $\boldsymbol{k} \parallel \boldsymbol{z}$, as depicted in Fig. 1(c). When the tilt angle is rotated to 90 degrees, the incident beam is parallel to the sample surface, $\boldsymbol{k} \perp \boldsymbol{z}$. and the magnetic field $\boldsymbol{H}$ penetrates through the ring. The orientation of electric field $\boldsymbol{E}$ was along the y-direction and the orientation of $\boldsymbol{E}$, $\boldsymbol{H}$ and $\boldsymbol{k}$ followed the right-handed rule. In the case of 90 deg of tilt angle, most of the power did not impinge on the sample because the sample (∼0.7 mm) was thinner than the diameter of the beam (∼4 mm), and the transmission measured by the detector was not below 0.7,

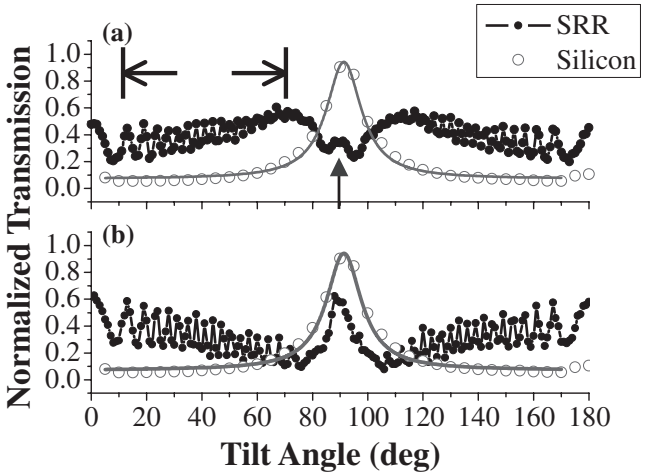

Fig. 2. Normalized transmission of the SRR cells when the tilt angle of sample is with respect to (a) the y-axis and (b) the x-axis. Data of planar the Al-coated Si substrate is presented for reference. The operating wavelength is 10.86 μm and the laser power on the sample is ∼100 mW.

increasing the detected transmitting power of P2. For comparison, planar Al-coated Si was used as a reference plate,where metallic Al had a thickness of ∼0.5 μm.

In Fig. 2 (a), when the tilt angle of the SSR sample was changed by 90 deg, the incident magnetic field penetrated through the SRR sample and the transmitted power dropped. Scattering and/or the absorption of the metal Al itself may cause transmission loss. But the effective ratio of the cross section of the metallic material to that of the Si substrate was so small ($\sim 5 \times 10^{-4}$) that the scattering effect could be neglected when the sample was rotated to θ=90°. Further-

more, the transmission loss caused by the scattering effect can be excluded, since the planar pure Al-coated Si substrate exhibited a higher transmission at θ=90° of around 0.9, as indicated by the curve of hollow circles in Fig. 2 (a). The transmission did not drop, but in fact peaked. Hence, the key factor of the drop must have been something else. The laser beam covered all the SRR cells in all tilt directions, so the absorption by the metal Al on the SRR cells should be the same as that for the pure Al on the reference sample, when metallic SRR cells form a bulk medium. However, this agreement was not observed. When the tilt angle approached 90 deg, the direct contribution of the incident beam to the detector became dominant, increasing the power detected on P2. For the case of planar pure Al-coated on Si, the evaluated value of detected power on P2 at 90 degrees was ~ 0.89, which was close to the experimental results represented by the curve of hollow circles in Fig. 2 (a). However, as shown in the curve of solid circles in Fig. 2 (a), the value of transmission did not increase, but dropped to approximately 0.3, as denoted by the upward arrows, implying that the interaction between SRR and the magnetic field is strong when the angle of tilt closes to 90 deg. The transmission drop must be caused by the SRR pattern. In other words, the magnetic field was significantly coupled to the SRR cell. Transmission loss is, therefore, *absorption* which occurs because of *resonance*.

Furthermore, the transmission drop cannot be considered as the diffraction of gratings. When the SRR patterns were considered as a diffraction grating, it must follow the grating equation, $\sin\theta_m - \sin\theta_0 = m(\lambda/d)$, where m represents the order of diffraction, θ_0 and θ_m are the angles of incidence and diffraction, respectively λ is the wavelength and d represents the period of the grating. The diffraction order higher than 1, i.e. $m \geqq 1$, was absent when the angle of incidence was around 90 deg. Restate, the detected power on P2 was not affected by the diffraction effect of the grating. The sample was also rotated to point along the x-axis, parallel to the optical table, such that the magnetic field did not penetrate through the SRR ring. However, the absorption disappeared, as shown in Fig. 2 (b), revealing that the relative orientation of the polarization is crucial. Essentially, the absorption mechanism is exactly the same as that in the case of *parallel polarization* described by Gay-Balmaz and Martin,[10] who used a mm-scale SRR cell and a GHz microwave source to demonstrate that *with parallel polarization, the incident magnetic field penetrates the SRR ring and thus generates a strong current that flows on the rings*. This feature also applies to the optical domain.

Consider the region of nonresonance at almost normal incidence, $\theta \sim 0$. Slightly changing the tilt angle leads to the significant variation of the transmission, unlike in the case of the Al-coated Si substrate, as can be seen in Fig. 2 (a). This variation, denoted by a pair of horizontal arrows ($\leftarrow \rightarrow$), was caused by the Fabry-Perot effect of the Si substrate. In other words, the outer interfaces of the Si plate acted as an etalon. For simplicity, the Fabry-Perot etalon is assumed to be an infinite plate with the transmission (T) as follows:

$$T = \frac{(1-R)^2}{(1-R)^2 + 4R\sin^2\sin^2\left(\dfrac{2\pi nL\cos\theta'}{\lambda_0}\right)}, \qquad (1)$$

where R, n, L and θ' represent the reflectance of the two interfaces, the refractive index, the thickness of the etalon and the angle of refraction of the etalon, respectively. However, pure Al-coated Si did not support the rapid oscillation, as shown in Fig. 2(a). This is because pure Al exhibited a large loss when light passed through the sample. The power decayed to approximately $\sim 10^{-19}$ for metal Al with $\sim 0.5\,\mu$m thickness. Consequently, the oscillation is suppressed when pure Al-coated Si is used. However, as the sample was rotated to 90 deg, the Fabry-Perot etalon effect would not occur and thus would not affect the resonance. A laser diode, in which the emission wavelength is 808 nm, and a He-Ne laser (wavelength 632.8 nm) were used to cross-check the rapid oscillation caused by the Fabry-Perot effect. Because the transmission of Si at wavelengths below 1 μm is extremely low, i.e. with a high loss, no rapid oscillation was observed, as shown in Fig. 3(b).

The relationship between the scales of SRR cells and the incident wavelength was also considered. We performed examinations at the incident wavelength smaller than the average size of a unit SRR cell, 9.43 μm and 808 nm, as shown in Fig. 3. The resonance of the SRR patterns also appeared in the case of the incident wavelength of 9.43 μm, as depicted in Fig. 3(a), but was absent at 808 nm which is much smaller than the SRR scale, as shown in Fig. 3(b). Notably, although the absorption of parallel polarization at 9.43 μm is less significant than that at 10.86 μm, it is still observable. In the case of 9.43 μm, one wavelength could not cover the entire SRR cell; however, the coherence of the laser light may improve the cooperation among the SRR cells, indicating that the maximum scale tolerance of the SRR pattern is around one wavelength of the incident beam.

In conclusion, a metallic planar wavelength-scale SRR is demonstrated to exhibit an absorption in the FIR wavelength range, of around $\sim 10.6\,\mu$m with parallel polarization. A reference experiment using a planar Al-coated Si sample is employed and compared to show the novel result. The absorption could be interpreted as "resonance". As in the cases in the microwave region, this resonance indicates negative permeability. Notably, the scale of the SRR pattern can be as high as one wavelength of the incident beam, the

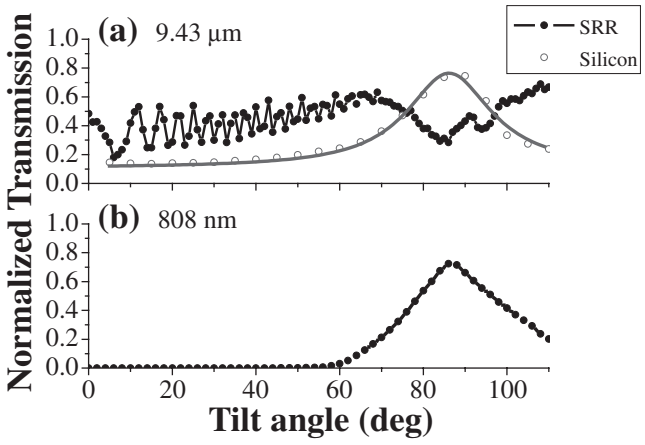

Fig. 3. Transmission through the SRR cells when the wavelength was (a) 9.43 μm, where the incident power on the sample was ~100 mW and the results of the planar Al-coated Si sample (empty circles) are also plotted for reference, and (b) 808 nm with ~30 mW incident power on the sample.

coherence of which may be critical to the onset of resonance. The experiment described herein demonstrates the resonance of SRR cells in the optical domain. This is important in the realization of NIR meta-materials in the optical wavelength domain.

We thank J.-S. Lih, M.-C. Chen, and Y.-C. Huang for the useful discussions and comments. The work of the NCTU group is partially supported by the National Science Council of Taiwan, R.O.C., under contract numbers NSC91-2112-M009-051 and NSC92-2112-M-009-040 and the Ministry of Economic Affairs of Taiwan, R.O.C., under contract number 91-EC-17-A-07-S1-0011.

1) J. B. Pendry: Phys. Rev. Lett. **85** (2000) 3966.
2) M. C. K. Wiltshire, J. B. Pendry, I. R. Young, D. J. Larkman, D. J. Gilderdale and J. V. Hajnal: Science **291** (2001) 849.
3) R. A. Shelby, D. R. Smith and S. Schultz: Science **292** (2001) 77.
4) D. Schurig and D. R. Smith: Appl. Phys. Lett. **82** (2003) 2215.
5) J. B. Pendry, A. J. Holden, W. J. Stewart and I. Youngs: Phys. Rev. Lett. **76** (1996) 4773.
6) J. B. Pendry, A. J. Holden, D. J. Robbins and W. J. Stewart: IEEE Trans. Microwave Theory & Tech. **47** (1999) 2075.
7) V. G. Vesslago: Sov. Phys. Usp. **10** (1968) 509.
8) J.-S. Lih, Y.-S. Wang, M.-C. Lu, M.-C. Chen, Y.-C. Huang, K.-H. Chen and J.-L. Chern: *Proc. Prog. Electromagnetic Research Symp. 2003* (Electromagnetics Academy, Cambridge, 2003) p. 96.
9) S. A. Tretyakov: Microwave & Opt. Tech. Lett. **31** (2001) 163.
10) P. Gay-Balmaz and O. J. F. Martin: J. Appl. Phys. **92** (2002) 2929.